Interplay of Pomeranchuk instability and superconductivity in the two-dimensional repulsive Hubbard model

Motoharu Kitatani, Naoto Tsuji, and Hideo Aoki

Phys. Rev. B **95**, 075109 — Published 3 February 2017

DOI: 10.1103/PhysRevB.95.075109

Interplay of Pomeranchuk instability and superconductivity in the two-dimensional repulsive Hubbard model

Motoharu Kitatani,[1] Naoto Tsuji,[2] and Hideo Aoki[1,3]

[1]*Department of Physics, University of Tokyo, Hongo, Tokyo 113-0033, Japan*
[2]*RIKEN Center for Emergent Matter Science (CEMS), Wako 351-0198, Japan*
[3]*Electronics and Photonics Research Institute, Advanced Industrial Science and Technology (AIST), Tsukuba, Ibaraki 305-8568, Japan*

(Dated: January 13, 2017)

Interplay of Pomeranchuk instability (spontaneous symmetry breaking of the Fermi surface) and d-wave superconductivity is studied for the repulsive Hubbard model on the square lattice with the dynamical mean field theory combined with the fluctuation exchange approximation (FLEX+DMFT). We show that the four-fold symmetric Fermi surface becomes unstable against a spontaneous distortion into two-fold near the van Hove filling, where the symmetry of superconductivity coexisting with the Pomeranchuk-distorted Fermi surface is modified from the d-wave pairing to $(d+s)$-wave. By systematically shifting the position of van Hove filling with varied second- and third-neighbor hoppings, we find that the transition temperature $T_c^{\rm PI}$ for the Pomeranchuk instability is more sensitively affected by the position of van Hove filling than the superconducting $T_c^{\rm SC}$. This implies that the filling region for strong Pomeranchuk instability and that for the $T_c^{\rm SC}$ dome can be separated, and that Pomeranchuk instability can appear even if the peak of $T_c^{\rm PI}$ is lower than the peak of $T_c^{\rm SC}$. An interesting finding is that the Fermi surface distortion can enhance the superconducting $T_c^{\rm SC}$ in the overdoped regime, which is explained with a perturbational picture for small distortions.

I. INTRODUCTION

High-Tc cuprate superconductors harbor many fundamental questions, which challenge elaborate numerical analysis on superconductivity, magnetism and other properties. Specifically, there is growing realization that various instabilities can exist along with superconductivity[1], and the relation between various charge instabilities and superconductivity in the cuprates is now being intensively studied[2–5]. Also, some experiments suggest a spontaneous breakdown of the four-fold symmetry of electronic states in the tetragonally structured cuprates, which is viewed as a kind of "electronic nematicity"[6–8]. There are some explanations for the nematicity, e.g. in the context of fluctuating stripe orders[9]. Pomeranchuk instability, a spontaneous breaking of four-fold symmetry of the Fermi surface without lattice distortion, is evoked as another possible candidate for nematicity in cuprate superconductors[10].

The presence of Pomeranchuk instability in two-dimensional lattice models has been suggested in Refs. 11,12, where the forward scattering was found to develop to induce Pomeranchuk instability. Subsequently, properties of this instability were studied primarily in mean-field models ("f-model"), where the electrons interact only via forward scattering[13,14]. For the two-dimensional (2D) Hubbard model on the square lattice, a representative model for cuprates, the existence of this instability is yet to be fully clarified microscopically. Functional renormalization group (fRG) calculations suggest that the superconducting fluctuation is stronger than Pomeranchuk instability[15], while other numerical renormalization-group approaches suggest Pomeranchuk instability to be stronger around van Hove fillings[16]. Gutzwiller wave functions combined with an efficient diagrammatic expansion technique (DE-GWF) obtained a ground state with a coexistence of the nematic order and superconductivity in 2D Hubbard model[17], which is also observed with the renormalized perturbation theory for the weak-coupling case[18]. Also, the dynamical cluster approximation (DCA) and cellular dynamical-mean-field theory (CDMFT) showed large responses against small distortions of the lattice[19,20], from which a possibility of spontaneous symmetry breaking is suggested to occur at lower temperatures or for larger cluster sizes. While these results suggest that the 2D repulsive Hubbard model has a strong tendency toward the Pomeranchuk instability, whether or not this instability has higher transition temperature ($T_c^{\rm PI}$) than that of superconductivity ($T_c^{\rm SC}$) has yet to be elaborated. More importantly, the relation between the Pomeranchuk instability and superconductivity (e.g., whether they are cooperative or competing) is an intriguing question. While a mean-field study for a phenomenological model suggests that they are competing with each other with $T_c^{\rm SC}$ suppressed in the coexistence region[21], the relation should be clarified by going beyond mean-field approaches.

Given the situation, we study in the present paper superconductivity and Pomeranchuk instability in the intermediate correlation regime by evoking FLEX+DMFT[22,23], a diagrammatic extension of the dynamical mean field theory (DMFT)[24–26], which takes account of the spin and charge fluctuation effects on top of the DMFT local self-energy, and can reproduce the dome structure in $T_c^{\rm SC}$[23]. The advantages of this method are first, there is no finite-size effects unlike in DCA and CDMFT, which should be important for capturing small Fermi surface deformations, and second, we can calculate finite-temperature regions in contrast to DE-GWF to capture the effect of this nematicity on the superconduct-

ing T_c^{SC}. This also enables us to systematically examine the relation between superconductivity and Pomeranchuk instability when the electron band filling and the second and further neighbor hoppings (t', t'') are varied. After confirming the existence of Pomeranchuk instability around the van Hove filling consistently with the previous works, we shall study the superconducting phase, which reveals that the symmetry of the gap function is changed from the ordinary d-wave pairing to $(d+s)$-wave[17,19]. Interestingly, the Fermi surface distortion can enhance the superconductivity in the overdoped (or strongly frustrated) regime with larger t', t''. We shall explain this T_c^{SC} enhancement with a perturbation picture for small Fermi-surface distortions, and also with the random phase approximation (RPA) in the weak-coupling regime.

Another finding here is that the Pomeranchuk instability temperature T_c^{PI} is more sensitive to (t', t''), hence the Fermi surface warping, than the superconducting T_c^{SC}. This contrasts with the previous mean-field calculations[21] that showed almost the same filling dependence for the two transition temperatures. This should come from the fact that the present formalism takes account of the filling dependence of the pairing interaction beyond mean-field levels. The result also implies that the superconducting T_c dome and that for Pomeranchuk instability can be separated.

II. FORMULATION

We consider the standard repulsive Hubbard model on the square lattice with a Hamiltonian,

$$\mathcal{H} = \sum_{\boldsymbol{k},\sigma} \epsilon(\boldsymbol{k}) c^\dagger_{\boldsymbol{k},\sigma} c_{\boldsymbol{k},\sigma} + U \sum_i n_{i,\uparrow} n_{i,\downarrow}, \tag{1}$$

where $c^\dagger_{\boldsymbol{k},\sigma}$ creates an electron with wave-vector $\boldsymbol{k} = (k_x, k_y)$ and spin σ, U is the on-site Coulomb repulsion, and $n_{i,\sigma} = c^\dagger_{i,\sigma} c_{i,\sigma}$. In the presence of second-neighbor (t') and third-neighbor (t'') hopping parameters, the 2D band dispersion is given as

$$\begin{aligned}\epsilon(\boldsymbol{k}) = &-2t(\cos k_x + \cos k_y) \\ &- 4t' \cos k_x \cos k_y - 2t''(\cos 2k_x + \cos 2k_y) - \mu,\end{aligned} \tag{2}$$

where t is the nearest-neighbor hopping (the unit of energy hereafter), and μ the chemical potential. We basically adopt $t' = -0.20t$, $t'' = 0.16t$, which are determined to fit the band calculation for a typical hole-doped single-layer cuprate, $HgBa_2CuO_{4+\delta}$[27,28].

For the numerical procedure, we employ FLEX+DMFT method, which is a kind of diagrammatic extension of DMFT, where the fluctuation exchange approximation (FLEX)[29] and the DMFT are combined with a double self-consistency loop. This kind of scheme has been considered in Refs.22,30, and has recently been formulated through Luttinger-Ward functional with applications to superconducting states in Ref.23. The latter can describe a T_c^{SC} dome against the band filling along with a spectral weight transfer. These are a virtue of FLEX+DMFT that corrects the overestimated local-FLEX self-energy in a filling-dependent manner. In FLEX+DMFT, the self-energy is calculated through the FLEX self-energy and DMFT self-energy ($\Sigma_{\rm imp}$) as

$$\Sigma(k) = \Sigma_{\rm FLEX}(k) - \Sigma^{\rm loc}_{\rm FLEX}(k) + \Sigma_{\rm imp}(\omega_n), \tag{3}$$

where the FLEX self-energy $\Sigma_{\rm FLEX}(k)$ is given as

$$\begin{aligned}\Sigma_{\rm FLEX}(k) = \frac{1}{N_k \beta} \sum_{k'} \Big[&\frac{3}{2} U^2 \frac{\chi_0(k-k')}{1 - U\chi_0(k-k')} \\ &+ \frac{1}{2} U^2 \frac{\chi_0(k-k')}{1 + U\chi_0(k-k')} - U^2 \chi_0(k-k') \Big] G(k').\end{aligned} \tag{4}$$

Here N_k and β are the total number of k-points and inverse temperature, respectively, $k \equiv (\omega_n, \boldsymbol{k})$ with ω_n the Matsubara frequency for fermions, $G(k)$ Green's function, and

$$\chi_0(q) = -\frac{1}{N_k \beta} \sum_k G(k+q) G(k) \tag{5}$$

is the irreducible susceptibility. The local part of the FLEX self-energy, $\Sigma^{\rm loc}_{\rm FLEX}$, is computed by replacing Green's function G with the local one, $G_{\rm loc} \equiv (1/N_k) \sum_{\boldsymbol{k}} G(k)$, in Eqs. (4) and (5).

For calculating the DMFT self-energy, $\Sigma_{\rm imp}$, we need to solve the impurity problem in DMFT. Here we employ the modified iterative perturbation theory (modified IPT) as the impurity solver. In this method, the original IPT is modified for the systems having no particle-hole symmetry[31], thus applicable to frustrated or non-half-filled cases. This is not computationally expensive, which enables us to scan over various parameter regions. We have checked, by using ALPS library[32,33], that the continuous-time quantum Monte Carlo (CT-QMC) impurity solver[34,35] gives similar results even away from half-filling in the intermediate-coupling regime [see Fig. 1(a)].

After obtaining Green's function, we plug it into the linearized Eliashberg equation,

$$\lambda \Delta(k) = -\frac{1}{N_k \beta} \sum_{k'} V_{\rm eff}(k-k') |G(k')|^2 \Delta(k'), \tag{6}$$

where $\Delta(k)$ is the anomalous self-energy, while

$$V_{\rm eff}(k) = U + \frac{3}{2} U^2 \frac{\chi_0(k)}{1 - U\chi_0(k)} - \frac{1}{2} U^2 \frac{\chi_0(k)}{1 + U\chi_0(k)} \tag{7}$$

is the effective pairing interaction, and λ the eigenvalue of Eliashberg's equation. Superconducting T_c^{SC} is determined as the temperature at which $\lambda = 1$. In the right-hand side of Eq. (6), we have neglected the local DMFT vertex contribution, whose validity is discussed in Appendix A.

To allow the Pomeranchuk instability to occur, we introduce a seed to deform the Fermi surface in the initial input for the self-energy as $\Sigma_{\rm initial} = 0.05t(\cos k_x - \cos k_y)$. While we linearize the anomalous part of Green's function as being infinitesimal, we can deal with finite Pomeranchuk order parameters, so that we can discuss superconductivity for finite distortions in this formalism.

III. RESULTS

A. Pomeranchuk instability

The Pomeranchuk order parameter η can be defined, for the originally four-fold cosine bands, as

$$\eta = \sum_{\boldsymbol{k}} (\cos k_y - \cos k_x) \left\langle c^\dagger_{\boldsymbol{k}} c_{\boldsymbol{k}} \right\rangle, \tag{8}$$

and we display the result against temperature and band filling in Fig. 1(a),(b), respectively. We can see that the order parameter starts to grow continuously with decreasing temperature, which indicates a second-order phase transition. If we turn to the filling dependence, we observe the order parameter abruptly grows around the edges of the Pomeranchuk phase, indicative of transferring to a first-order phase transition consistently with the previous work[13]. Hereafter, we focus on the filling region around the peak of $T_{\rm c}^{\rm PI}$, where the transition is of second order.

If we look at the Fermi surface in Fig. 1(c) for $U/t = 4.0$ and $n = 0.66$, we can see that the Fermi surface, identified as the ridges in the spectral function $A(\boldsymbol{k}, \omega = 0)$ obtained with the Padé approximation, indeed becomes distorted at lower temperatures, $T < T_{\rm c}^{\rm PI}$.

The phase diagram is displayed in Fig. 2(a), where we can see that the Pomeranchuk instability temperature $T_{\rm c}^{\rm PI}$, which is determined as the temperature at which η becomes nonzero, is peaked around $n = 0.66$ for the present parameter set $(U/t = 4.0, (t', t'') = (-0.20, 0.16))$. An yellow arrow indicates the van Hove filling in the interacting system at which the spectrum is peaked at the Fermi energy, see Fig. 2(b), in which we have obtained the density of states with the Padé approximation and confirmed the peak position does not change for $T > T_{\rm c}^{\rm PI}$. The fact that the Pomeranchuk instability tends to be strong near this filling is consistent with the previous results[13,21]. The peak in the Pomeranchuk dome does not precisely coincide with the van Hove filling, which may be an effect of the asymmetric density of states[13] as in Fig. 2(b). By contrast, the superconducting $T_{\rm c}^{\rm SC}$ in the present result is a monotonically decreasing function of the hole doping around the van Hove filling.

This contrasts with the previous mean-field calculations[21] which ignore the filling dependence of the effective pairing interaction, where both $T_{\rm c}^{\rm SC}$ and $T_{\rm c}^{\rm PI}$ are peaked around the van Hove filling. Thus the present result indicates that the filling dependence

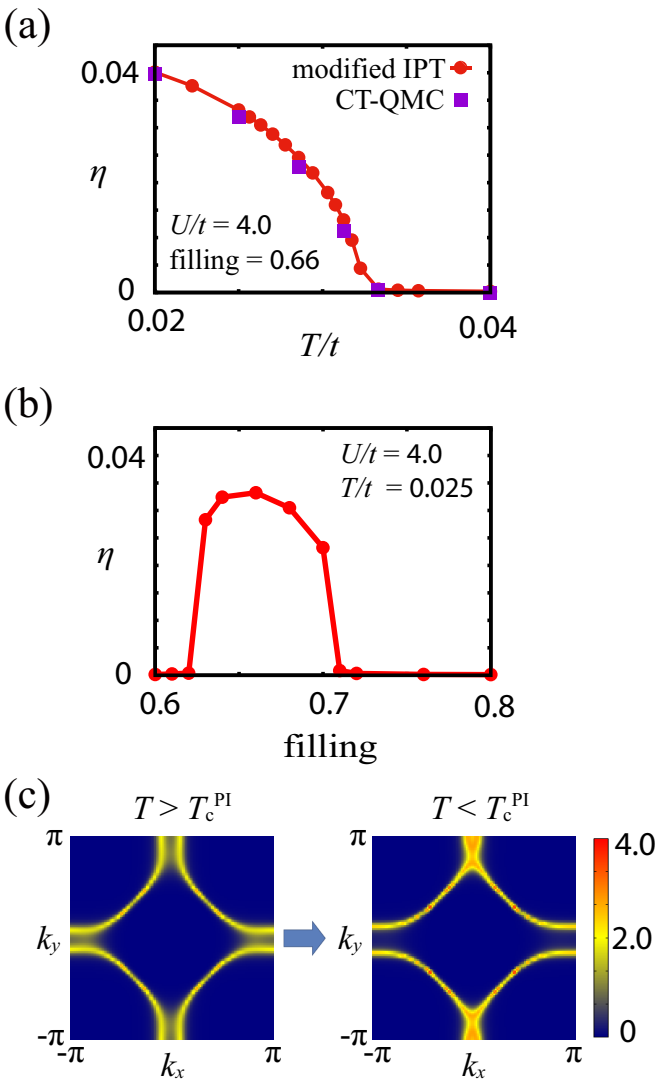

FIG. 1: (Color online) (a) Temperature dependence and (b) filling dependence of the Pomeranchuk order parameter η for $U/t = 4.0, (t', t'') = (-0.20, 0.16)$. In (a), the circles (squares) represent the results of FLEX+DMFT with the modified IPT (CT-QMC) as a DMFT impurity solver. (c) Fermi surface [as represented by the color-coded spectral weight $A(\boldsymbol{k}, \omega = 0)$] with $n = 0.66, U/t = 4.0, (t', t'') = (-0.20, 0.16)$, for $T = 0.0333t > T_{\rm c}^{\rm PI}$ ($\beta t = 30$; left) and $T = 0.0286t < T_{\rm c}^{\rm PI}$ ($\beta t = 35$; right).

of the effective interaction has an important effect of rendering distinction of optimal doping levels between Pomeranchuk $T_{\rm c}^{\rm PI}$ dome and superconducting $T_{\rm c}^{\rm SC}$ dome. To confirm this, let us systematically vary the second- and third-neighbor hopping parameters (t', t'') in Fig. 3, which change the Fermi surface warping as well as the van Hove filling. We can see that, for a fixed $n = 0.80$, the change in the parameters shifts the distance of the filling from the van Hove filling as represented by the blurring of the spectral function around $(0, \pi), (\pi, 0)$. Left panels in Fig. 3 plot the phase diagrams for three

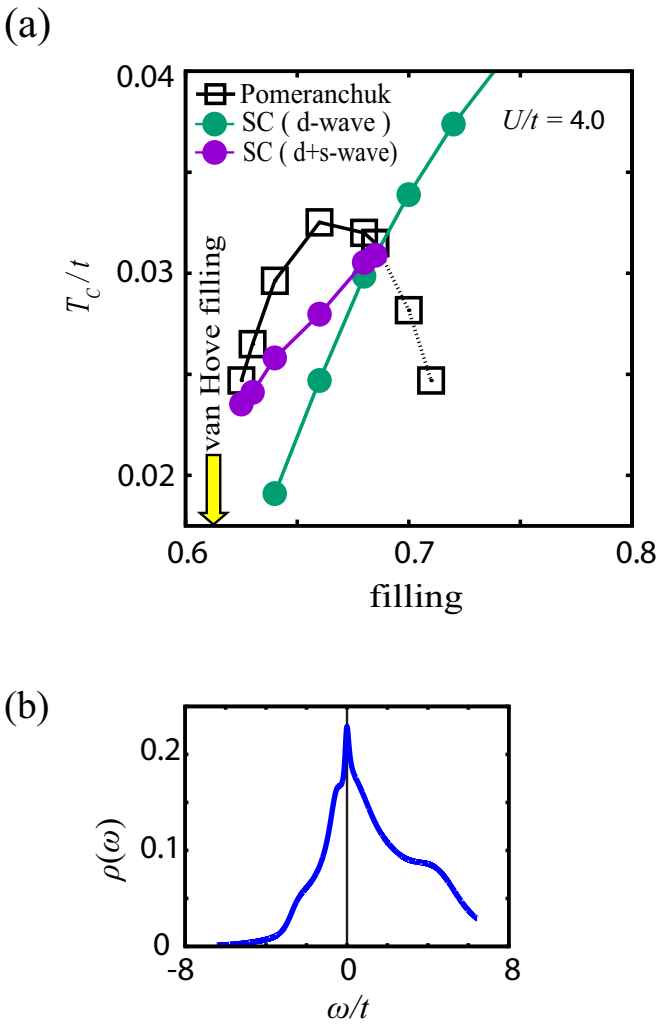

FIG. 2: (Color online) (a) Phase diagram against temperature T/t and band filling n for $U/t = 4.0, (t', t'') = (-0.20, 0.16)$. Shown are the superconducting $T_c^{\rm SC}$ with undistorted Fermi surface (green circles), superconducting $T_c^{\rm SC}$ with Fermi surface distortion (purple circles), and Pomeranchuk $T_c^{\rm PI}$ (black squares). The dotted line represents $T_c^{\rm PI}$ when we ignore the superconductivity. The yellow arrow indicates the van Hove filling in the interacting system. (b) Density of states at the filling indicated by the yellow arrow in (a) for $\beta t = 20, U/t = 4.0, (t', t'') = (-0.20, 0.16)$.

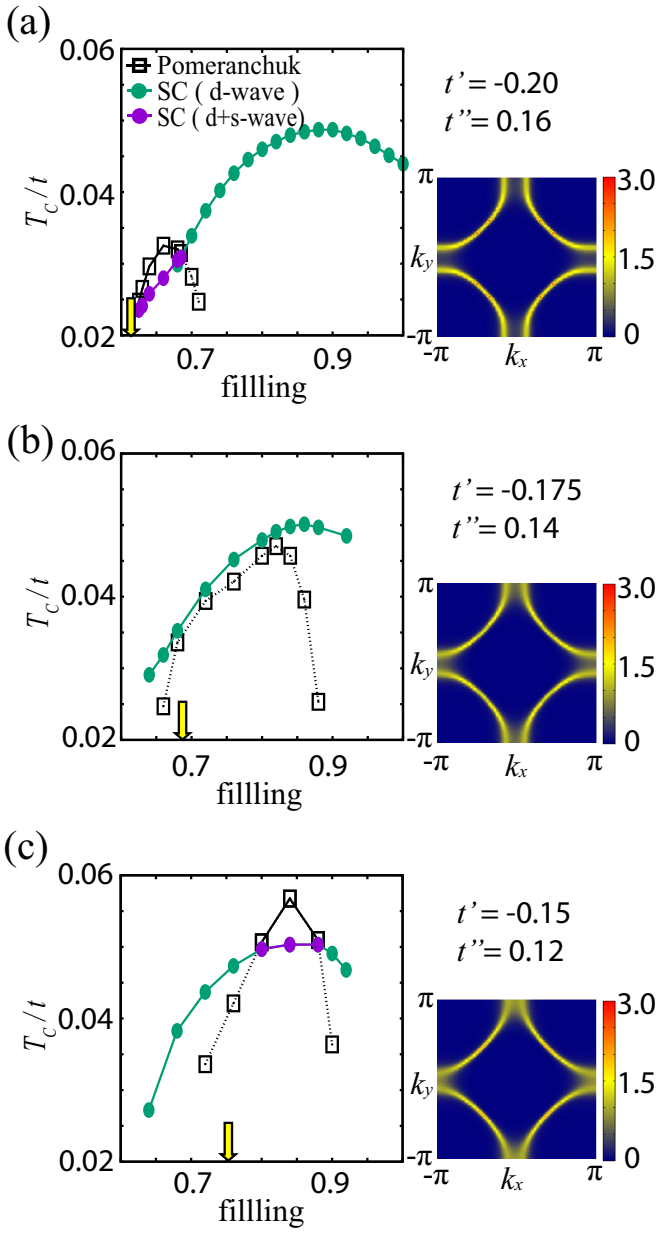

FIG. 3: (Color online) The superconducting and Pomeranchuk phase boundaries for $U/t = 4.0$ (left panels) and the spectral weight $A(\boldsymbol{k}, \omega = 0)$ for $n = 0.80, \beta t = 20, U/t = 4.0$ (right) are shown for $(t', t'') = (-0.20, 0.16)$ (a), $(-0.175, 0.14)$ (b), and $(-0.15, 0.12)$ (c). The symbols are the same as in Fig. 2(a), and yellow allows indicate respective van Hove fillings in the interacting system.

typical cases with different Fermi surface warping. We find that the Pomeranchuk $T_c^{\rm PI}$ drastically changes along with the van Hove filling (yellow allows), while the superconducting $T_c^{\rm SC}$ is much less sensitive.

We can thus conclude that, despite both of superconductivity and Pomeranchuk instability being Fermi surface instabilities affected by the spectral weight at the Fermi energy, the Pomeranchuk instability is much more sensitive to the Fermi surface shape (distance from the van Hove filling). This implies that we can separate the dominant regions for the two instabilities by changing the position against the van Hove filling (dominated by t', t'').

B. Superconductivity under Fermi surface distortions

Now, an intriguing issue is how superconductivity behaves in the presence of the Pomeranchuk Fermi-surface

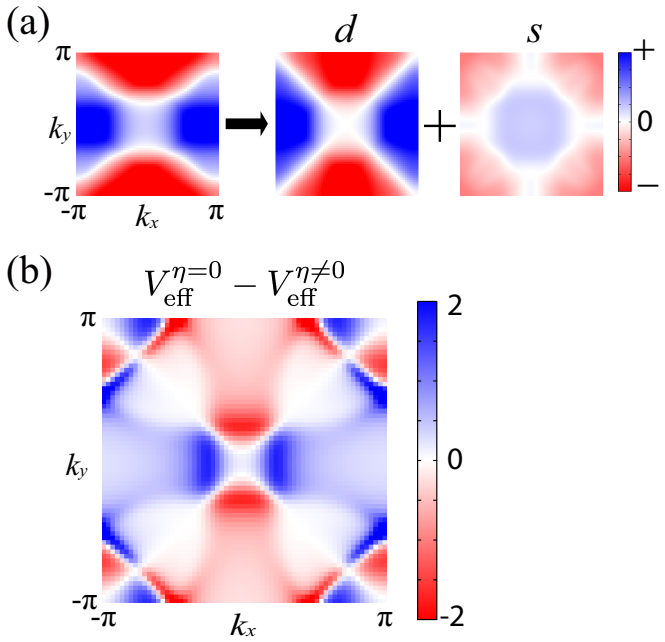

FIG. 4: (Color online) (a) Momentum dependence of the gap function for $T = 0.0286t < T_c^{\rm PI}$ with $n = 0.66, U/t = 4.0, (t', t'') = (-0.20, 0.16)$ (left panel), which can be decomposed into a d-wave part and an (extended) s-wave (four-fold symmetric) part (right). (b) Difference in the pairing interaction with the Fermi surface distortion ($V_{\rm eff}^{\eta\neq0}$) and without ($V_{\rm eff}^{\eta=0}$), for $n = 0.66, \beta t = 31, U/t = 4.0, (t', t'') = (-0.20, 0.16)$.

distortion. If we look at the superconducting order parameter in Fig. 4(a), the pairing symmetry is seen to be distorted from the ordinary d-wave to d+(extended)s-wave. Here, an interesting observation is that the superconducting $T_{\rm c}^{\rm SC}$ can be *enhanced* by the Pomeranchuk distortion of the Fermi surface. Indeed, if we go back to Fig. 2, we have also plotted the superconducting $T_{\rm c}^{\rm SC}$ (green dots) when the four-fold Fermi surface is artificially imposed below Pomeranchuk $T_{\rm c}^{\rm PI}$. We can see the $T_{\rm c}^{\rm SC}$ with the distorted Fermi surface (purple dots) is actually higher.

To identify the origin of this enhancement, we can compare the pairing interaction between the cases of Pomeranchuk-distorted and the four-fold-imposed Fermi surfaces. Figure 4(b) plots the difference of the two cases for the same parameters ($U/t = 4.0$, $n = 0.66$ and $\beta t = 31$). We can see that the Pomeranchuk instability distorts the pairing interaction, where the difference has a d-wave-like sign reversal.

To pin-point the origin of the distortion effect on the superconducting $T_{\rm c}^{\rm SC}$, we can consider the perturbational effect for small distortions, based on a general linearized gap equation,

$$\lambda\phi(k) = -\frac{1}{N_k\beta}\sum_{k'} K(k,k')\phi(k'), \tag{9}$$

where $\phi(k) = |G(k)|\Delta(k)$, while $K(k,k')$ is the kernel, given as $K(k,k') = |G(k)|V_{\rm eff}(k-k')|G(k')|$ in FLEX+DMFT (as seen by multiplying $|G|$ to both sides of Eq. (6)). If we consider small d-wave-like distortions [as displayed in Fig. 4(b)] for this kernel,

$$K(k,k') \to K(k,k') + \delta K^{\rm d}(k,k'), \tag{10}$$

the first-order perturbation for the maximum eigenvalue $\lambda_{\rm max}$ satisfies

$$\delta\lambda_{\rm max}^{(1)} = \sum_{k,k'} \phi_{\rm max}^*(k)\delta K^{\rm d}(k,k')\phi_{\rm max}(k') = 0, \tag{11}$$

where $\phi_{\rm max}$ is the eigenvector for $\lambda_{\rm max}$. Namely, $\delta\lambda_{\rm max}^{(1)}$ identically vanishes due to the d-wave nature of the $\delta K^{\rm d}$, so that the leading term is the second-order one,

$$\delta\lambda_{\rm max}^{(2)} = \sum_{i,k,k'} \frac{|\phi_{\rm max}^*(k)\delta K^{\rm d}(k,k')\phi_i(k')|^2}{\lambda_{\rm max}-\lambda_i} > 0, \tag{12}$$

where i is the index for the eigenvalue λ_i and eigenvector ϕ_i of the kernel matrix K. Since this expression is positive-definite, small d-wave deformations of the kernel in the linearized gap equation always enhance the superconducting $T_{\rm c}^{\rm SC}$. This explains the $T_{\rm c}^{\rm SC}$ enhancement in Fig. 2(a), and can provide a new pathway for enhancing superconducting $T_{\rm c}^{\rm SC}$ in terms of Fermi surface distortion.

However, it should be difficult to achieve purely d-wave like distortions for the kernel, and the terms having some other symmetries should in general arise even from purely d-wave distortions of the Fermi surface. We can elaborate this by introducing a parameter g_k, where g_k represents either (i) a spontaneous distortion of the electronic states [$\delta g_k = G(k) - G_{\rm undistorted}(k)$], or (ii) a small d-wave modulation of the Hamiltonian ($\delta\mathcal{H} = \sum_{\boldsymbol{k},\sigma} \delta g_k c_{\boldsymbol{k},\sigma}^\dagger c_{\boldsymbol{k},\sigma}$). Then we can expand the interaction kernel in g_k, which gives, up to the second-order,

$$K(k,k') \to K(k,k') + \sum_p \frac{\delta K}{\delta g_p}\delta g_p + \frac{1}{2}\sum_{p,q}\frac{\delta^2 K}{\delta g_p \delta g_q}\delta g_p \delta g_q, \tag{13}$$

and the effect on the eigenvalue λ reads

$$\delta\lambda_{\rm max}^{(2)} = \sum_{i,k,k'} \frac{|\phi_{\rm max}^*(k)\sum_p \frac{\delta K}{\delta g_p}\delta g_p \phi_{\rm i}(k')|^2}{\lambda_{\rm max}-\lambda_{\rm i}} - \sum_{k,k'}\phi^*(k)\frac{1}{2}\sum_{p,q}\frac{\delta^2 K}{\delta g_p \delta g_q}\delta g_p \delta g_q \phi(k'). \tag{14}$$

We can see that whether $T_{\rm c}^{\rm SC}$ can be enhanced depends on the second term on the right-hand side of Eq. (14). From this we expect that the enhancement tends to occur when the *second-largest* eigenvalue is close to the largest one, for which the first term on the right-hand side of Eq. (14) becomes dominant.

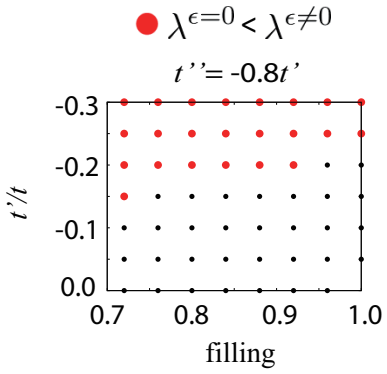

FIG. 5: (Color online) Comparison of the eigenvalue λ calculated with RPA between the four-fold symmetric Fermi surface ($\epsilon = 0$) and the distorted Fermi surface ($\epsilon = 0.01$) with red (black) dots representing the case of $\lambda^{\epsilon=0} < \lambda^{\epsilon=0.01}$ ($\lambda^{\epsilon=0} > \lambda^{\epsilon=0.01}$) for $\beta t = 5, U/t = 2.0$. The horizontal axis corresponds to the band filling, while the vertical axis is t'/t, with $t'' = -0.8t'$ (which includes the parameter set used in Fig. 3).

We can in fact check this argument in the weak-coupling case. To obtain qualitative tendencies, we have performed a RPA calculation at a relatively high temperature for various values of parameters to compare the four-fold symmetric case with the distorted Fermi surface by making the nearest-neighbor hopping slightly anisotropic, $t_x = 1 + \epsilon, t_y = 1 - \epsilon$, by hand with the first line in Eq. (2) becoming $\epsilon(\boldsymbol{k}) = -2t_x \cos k_x - 2t_y \cos k_y$. In the RPA, we ignore the self-energy effect in the Eliashberg Eq. (6).

When we compare the eigenvalue under a distortion $\lambda^{\epsilon=0.01}$ with $\lambda^{\epsilon=0}$ for the symmetric case, the result in Fig. 5 for $U/t = 2.0, \beta t = 5$ shows that we do have a region (marked with red circles representing $\lambda^{\epsilon=0.01} > \lambda^{\epsilon=0}$) in which the distortion enhances the eigenvalue. This effect tends to occur away from half-filling, and for larger values of distant-neighbor hopping t', t'' (i.e., more frustrated cases). Thus we can confirm that the enhancement of the superconductivity by small distortions indeed occurs in the weak-coupling limit where we can ignore the self-energy effect.

It has been known that the gap symmetry (for the leading eigenvalue) tends to be changed for higher doping or more frustrated cases[36]. The present result suggests that the T_c^{SC} enhancement arising from the distortion tends to occur around the boundary for the gap symmetry to change where the leading and sub-leading eigenvalues are close to each other. This is also consistent with the above result for the t' dependence in FLEX+DMFT (Fig. 3), where the enhancement of T_c^{SC} occurs for $(t', t'') = (-0.20, 0.16)$. We also notice that the structure of Eq. (14) is reminiscent of the pseudo Jahn-Teller effect, in which a Jahn-Teller-like distortion occurs without degeneracies due to the second-order effect of the distortion[37]. In this context we can also recall a well-known property that, if the eigenvalues are degenerate (e.g. for $p + ip$-pairing), T_c^{SC} can be enhanced by the strain effect[38]. From these, the present result may also be viewed as a possibility for this kind of T_c^{SC} enhancement revealed even for the (non-degenerate) d-wave regime in 2D square lattice Hubbard model.

IV. SUMMARY AND DISCUSSIONS

We have employed FLEX+DMFT approach to study the interplay of Pomeranchuk instability and superconductivity in correlated electron systems. We have revealed that the superconductivity with the distorted Fermi surface has the symmetry of the gap function changed from d-wave to $d + s$, consistent with the previous studies[17,19]. We have found that the Fermi surface distortion can enhance the superconducting T_c^{SC} in the overdoped regime. We have explained this enhancement in terms of the perturbation for small distortions, and also with RPA in the weak-coupling regime. The Pomeranchuk T_c^{PI} is found to be much more sensitive to Fermi surface warping and the position of the van Hove filling than the superconducting transition temperature.

In the main parameter set for the present calculation, the Pomeranchuk T_c-dome appears in the overdoped region, while experimentally the electronic nematicity is mainly observed in the underdoped regime. If the nematicity in the cuprates comes from the Pomeranchuk instability, then the present result suggests that it should strongly depend on the component materials that can have various values of second- (t') and third-neighbor (t'') hoppings: For instance, $La_{2-x}Sr_xCuO_4$ with smaller t', t'' has the van Hove filling sitting around 20% doping[28,39,40], which is close to the situation given in Fig. 3(c), where the Pomeranchuk T_c-dome appears around the optimal to underdoped regimes.

If we comment on the method, FLEX+DMFT, despite being an improvement over FLEX or DMFT, still overestimates the non-local self-energy effect. For more accurate estimates, other methods (e.g. diagrammatic expansion in two-particle level as in DΓA[41] or dual fermion method[42]) will be needed. Also, we have assumed here translationally invariant systems, while the study of the interplay between superconductivity and charge instabilities involving finite wave vectors will be another interesting future work.

V. ACKNOWLEDGEMENT

The present work was supported by JSPS KAKENHI Grant Number JP26247057, and by ImPACT Program of Council for Science, Technology and Innovation, Cabinet Office, Government of Japan (No. 2015- PM12-05-01) (HA), and by the Advanced leading graduate course for photon science (MK), and by JSPS KAKENHI Grant Number JP25800192 (NT).

Appendix A: Effect of the DMFT vertex $\Gamma_{\rm DMFT}$

According to the formulation in Ref.23, we should consider the local anomalous self-energy $\Delta_{\rm loc}$ coming from the DMFT functional. Then the linearized Eliashberg equation becomes

$$\lambda\Delta(k) = -\frac{1}{N_k\beta}\sum_{k'}[V_{\rm eff}(k-k') + \Gamma_{\rm DMFT}(\omega_n,\omega_m)] \times |G(k')|^2\Delta(k'), \quad \text{(A1)}$$

where $\Gamma_{\rm DMFT} = \delta\Delta_{\rm loc}/\delta F$ is the functional derivative of the local anomalous self-energy. While this term can be ignored for studying pure d-wave pairing as in the previous paper[23], we examine its effect on the $d+s$ pairing here. We consider this effect to be small, because the additional term is an extended s-wave (nonlocal) pairing rather than the ordinary s-wave, so that a cancellation should occur in the momentum summation. To check this along the argument in the main text, we can calculate the lower bound for the maximal eigenvalue when $\Gamma_{\rm DMFT}$ is considered without calculating $\Gamma_{\rm DMFT}$ directly. From the eigenvector $\Delta_{\rm max}$ of Eq. (6), we extract the part of the gap function that is not affected by $\Gamma_{\rm DMFT}$ as

$$\Delta'(k) = \Delta_{\rm max}(k) - \frac{\sum_{\boldsymbol{k}}|G(k)|^2\Delta_{\rm max}(k)}{\sum_{\boldsymbol{k}}|G(k)|^2}. \quad \text{(A2)}$$

Then a quantity,

$$\lambda' = -\frac{\sum_{k,k'}\Delta'^*(k)|G(k)|^2V_{\rm eff}(k-k')|G(k')|^2\Delta'(k')}{\sum_k\Delta'^*(k)|G(k)|^2\Delta(k)}, \quad \text{(A3)}$$

gives the lower bound for the maximal eigenvalue when $\Gamma_{\rm DMFT}$ is considered. We have actually confirmed that the difference between λ' and λ (without $\Gamma_{\rm DMFT}$) is very small, $(\lambda-\lambda')/\lambda < 0.01$. Thus we can conclude the effect of the DMFT vertex $\Gamma_{\rm DMFT}$ does not significantly change the the result for the $T_{\rm c}^{\rm SC}$ enhancement.

[1] B. Keimer, S. A. Kivelson, M. R. Norman, S. Uchida and J. Zaanen, Nature **518**, 179 (2015).
[2] T. Wu, *et al.*, Nature **477**, 191 (2011).
[3] E. H. da Silva Neto, *et al.*, Science **343**, 393 (2014).
[4] R. Comin, *et al.*, Science **343**, 390 (2014).
[5] W. Tabis, *et al.*, Nature Commun. **5**, 5875 (2014).
[6] Y. Ando, K. Segawa, S. Komiya, A. N. Lavrov, Phys. Rev. Lett. **88**,137005 (2002).
[7] V. Hinkov, *et al.*, Science **319**, 597 (2008).
[8] M. J. Lawler, *et al.*, Nature **466**, 347 (2010).
[9] S.A. Kivelson, E. Fradkin, and V. J. Emery, Nature (London) **393**, 550 (1998).
[10] H. Yamase and W. Metzner, Phys. Rev. B **73**, 214517 (2006).
[11] C. J. Halboth and W. Metzner, Phys. Rev. Lett. **85**,5162 (2000).
[12] H. Yamase and H. Khono, J. Phys. Soc. Jpn. **69**, 332 (2000).
[13] H. Yamase, V. Oganesyan and W. Metzner, Phys. Rev. B **72**, 035114 (2005).
[14] P. Jakubczyk, W. Metzner and H. Yamase, Phys. Rev. Lett. **103**,220602 (2009).
[15] C. Honerkamp, M. Salmhofer and T. M. Rice, Eur. Phys. J. B **27**, 127 (2002).
[16] V. Hankevych, I. Grote and F. Wegner, Phys. Rev. B **66**, 094516 (2002).
[17] J. Kaczmarczyk, T. Schickling and J. Bunemann, arXiv:1512.06688.
[18] A. Neumayr and W. Metzner, Phys. Rev. B **67**, 035112 (2003).
[19] S. Q. Su and T. A. Maier, Phys. Rev. B **84**, 220506(R) (2011).
[20] S. Okamoto, D. Senechal, M. Civelli and A. M. S. Tremblay, Phys. Rev. B **82**, 180511(R) (2010).
[21] H. Yamase and W. Metzner, Phys. Rev. B **75**, 155117 (2007).
[22] J. Gukelberger, L. Huang, and P. Werner, Phys. Rev. B **91**, 235114 (2015).
[23] M. Kitatani, N. Tsuji and H. Aoki, Phys. Rev. B **92**, 085104 (2015).
[24] W. Metzner and D. Vollhardt, Phys. Rev. Lett. **62**,324 (1989).
[25] A. Georges and G. Kotliar, Phys. Rev. B **45**, 6479 (1992).
[26] A. Georges, G. Kotliar, W. Krauth, and M. J. Rozenberg, Rev. Mod. Phys. **68**, 13 (1996).
[27] K. Nishiguchi, K. Kuroki, R. Arita, T. Oka, and H. Aoki, Phys. Rev. B **88**, 014509 (2013); K. Nishiguchi, PhD Thesis Univ. of Tokyo (2013).
[28] Similar values are also obtained in H. Sakakibara, H. Usui, K. Kuroki, R. Arita, and H. Aoki, Phys. Rev. Lett. **105**,057003 (2010); Phys. Rev. B **85**, 064501 (2012), where single- vs two-orbital models are examined.
[29] N. E. Bickers, D. J. Scalapino and S. R. White, Phys. Rev. Lett. **62**,8 (1989).
[30] J. P. Hague, M. Jarrell, and T. C. Schulthess, Phys. Rev. B **69**, 165113 (2004).
[31] H. Kajueter and G. Kotliar, Phys. Rev. Lett. **77**,131 (1996).
[32] B. Bauer, *et al.*, J. Stat. Mech. P05001 (2011).
[33] A. F. Albuquerque, *et al.*, J. Magn. Magn. Mater. **310**, 1187 (2007).
[34] A. N. Rubtsov, V. V. Savkin, and A. I. Lichtenstein, Phys. Rev. B **72**, 035122 (2005).
[35] E. Gull, A. J. Millis, A. I. Lichtenstein, A. N. Rubtsov, M. Troyer, and P. Werner, Rev. Mod. Phys. **83**, 349 (2011).
[36] A. T. Rømer, *et al.*, Phys. Rev. B **92**, 104505 (2015).
[37] U. Opik, and M. H. L. Pryce, Proc. Roy. Soc. London Ser. A **238**, 425 (1957).
[38] M. B. Walker, and P. Contreras, Phys. Rev. B **66**, 214508 (2002).
[39] A. Ino, *et al.*, Phys. Rev. B **65**, 094504 (2002).
[40] T. Yoshida, *et al.*, Phys. Rev. B **74**, 224510 (2006).
[41] A. Toschi, A. A. Katanin, and K. Held, Phys. Rev. B **75**, 045118 (2007).

[42] A. N. Rubtsov, M. I. Katsnelson, and A. I. Lichtenstein, Phys. Rev. B **77**, 033101 (2008).